ELSEVIER

Journal of Molecular Catalysis A: Chemical 138 (1999) 177–184

JOURNAL OF MOLECULAR CATALYSIS A: CHEMICAL

A study on reduction behaviors of the supported platinum–iron catalysts

Jifei Jia [a,*], Jianyi Shen [b], Liwu Lin [a], Zhusheng Xu [a], Tao Zhang [a], Dongbai Liang [a]

[a] *Dalian Institute of Chemical Physics, Chinese Academy of Sciences, P.O. Box 110, Dalian 116023, China*
[b] *Department of Chemistry, Nanjing University, Nanjing 210093, China*

Received 25 November 1997; accepted 26 March 1998

Abstract

The reduction behaviors of the supported platinum–iron catalysts and their comparison with supported iron catalysts were studied by TPR (temperature-programmed reduction)–in situ ^{57}Fe MBS (Mössbauer spectroscopy). The results indicated that the TPR processes of all Fe-containing catalysts were different from that of bulk α-Fe_2O_3. There were interactions between Pt, Fe and the γ-Al_2O_3 or SiO_2 support for the Pt–Fe/γ-Al_2O_3 and Pt–Fe/SiO_2 catalysts. All the iron-containing catalysts show that Fe^{3+} was highly dispersed on the support (γ-Al_2O_3 and SiO_2) before reduction. No Fe^0 was found in the reduction processes. The Fe^{3+} was reduced to Fe^{2+} in tetrahedral vacancy first for the reduction of the Pt–Fe/γ-Al_2O_3 catalyst. No Fe^{2+} in octahedral vacancy was found in the reduction of the Pt–Fe/SiO_2 catalyst. Adding Pt to Fe/support (γ-Al_2O_3 or SiO_2) could promote the reduction of the Fe species.

Keywords: Pt; Fe; TPR; In situ Mössbauer spectroscopy

1. Introduction

For the last three decades, Pt-containing bimetallic catalysts have been widely used in the petroleum industry for reforming, dehydrogenation and hydrogenation reactions [1,2]. In the early studies, due to the strong influence of catalytic theory of alloys [3] and the limitations of characterization techniques, the states of the two highly dispersed catalytic components in a bimetallic catalyst were usually considered to exist as an alloy or bimetallic clusters [4]. Recently, with the development of highly sensitive and in situ physical techniques for the characterization of catalysts, it has been reported that, for alumina supported bimetallic catalysts, due to the strong interaction between the catalytic components and the support, only one of the components is in the metallic state, while the other component still remains in the oxidation states after reduction. For example, the Re, Ge, and Sn components in Pt–Re/Al_2O_3 [5,6], Pt–Ge/Al_2O_3 [7] and Pt–Sn/Al_2O_3 [8–11] catalysts could not be reduced to the zero oxidation state after reduction at elevated temperatures, while the Pt component was in the metallic state. The temperature-programmed reduction (TPR) [12] technique can provide information of the dispersion states of the metallic components, as well as the extent of metal–support and metal–metal interactions in metallic catalysts. However, it is not easy to identify each of the

* Corresponding author.

1381-1169/99/$ - see front matter
PII: S1381-1169(98)00147-2

reduction peaks in a TPR profiles. In this regard Mössbauer spectroscopy (MBS) is a powerful technique which can determine the chemical states of various species in a catalyst under in situ conditions. Thus, a combined in situ TPR–MBS technique [13,14] is an ideal means for the characterization of the bimetallic catalysts. Our previous studies [15] indicated that Pt–Fe bimetallic catalysts, supported either on γ-Al_2O_3 with a 5:1 Fe/Pt atomic ratio, or on SiO_2 with a 2:1 Fe/Pt atomic ratio, are promising catalysts for the dehydrogenation of alkanes. Although extensive studies have been done for supported Fe and Pt–Fe system [13,14,16–19], very few information have been reported on combined TPR–MBS investigations. In this work a combined in situ TPR–MBS technique was employed to investigate the reduction process of γ-Al_2O_3 and SiO_2 supported Pt–Fe catalyst, and compared their results with that of the corresponding supported Fe catalysts.

2. Experimental

2.1. Preparation of the catalysts

The γ-Al_2O_3 or SiO_2 supported Pt or Fe mono metallic catalysts were prepared by impregnating the γ-Al_2O_3 (surface area: 156 m^2/g) or SiO_2 (surface area: 440 m^2/g) supports with $H_2PtCl_6 \cdot 6H_2O$ or $Fe(NO_3)_3 \cdot 9H_2O$ aqueous solutions, with 2% HCl added as a competing adsorbate. The Pt–Fe/γ-Al_2O_3 and Pt–Fe/SiO_2 bimetallic catalysts were prepared by the sequential impregnation method. For this, the Fe/support catalyst precursor was first prepared by impregnating with an $Fe(NO_3)_3$ aqueous solution, then dried and calcined. Subsequently, the Pt–Fe/support catalyst was prepared by impregnating with a H_2PtCl_6 aqueous solution, then dried and calcined again. Drying processes for all catalysts were at 60°C for 4 h followed by 120°C for another 4 h. After drying, the catalysts were calcined at 480°C in air for 4 h, then calcined in steam for another 4 h to remove the chloride ions. In all platinum-containing samples, the Pt content was 0.375 wt.%. The Fe content was 0.537 wt.% (Fe/Pt of 5:1 atomic ratio) for the γ-Al_2O_3 supported catalysts and 0.215 wt.% (Fe/Pt of 2:1 atomic ratio) for the SiO_2 supported catalysts. A total of 0.1 wt.% of the ^{57}Fe isotope was added in all iron-containing samples for MBS determinations.

2.2. TPR measurements

A schematic diagram of the temperature-programmed apparatus has been described in Ref. [16]. The measurements were performed in a quartz tube with a N_2–H_2 (7.63 mol% H_2) gas mixture at a flow rate of 20 ml/min. The heating rate was 10 K/min. The weight of the samples used for each measurement was 0.200 $\pm$ 0.001 g.

2.3. In situ combined TPR–MBS

The in situ combined TPR–MBS was carried out in a quartz Mössbauer absorber cell [14]. At first, according to the experimental conditions required by the MBS, an integrated TPR profile was measured. Then for each peak on the TPR profile, the temperature was raised up to the peak position and then the temperature-programming was stopped when the peak was completed; and the sample was cooled immediately in a N_2–H_2 stream to ambient temperature for Mössbauer measurement. A 15 mCi $^{57}Co(Pd)$ source was used. All spectra were computer-fitted to a Lorentzian line shape using a least-squares fitting procedure. The velocity of the MBS was calibrated by the distance between lines 3 and 4 of the α-Fe spectrum [14].

3. Results and discussion

3.1. TPR spectra studies

The TPR profiles of γ-Al_2O_3, Fe/γ-Al_2O_3, Pt/γ-Al_2O_3 and Pt–Fe/γ-Al_2O_3 samples are given in Fig. 1. Only one reduction peak at

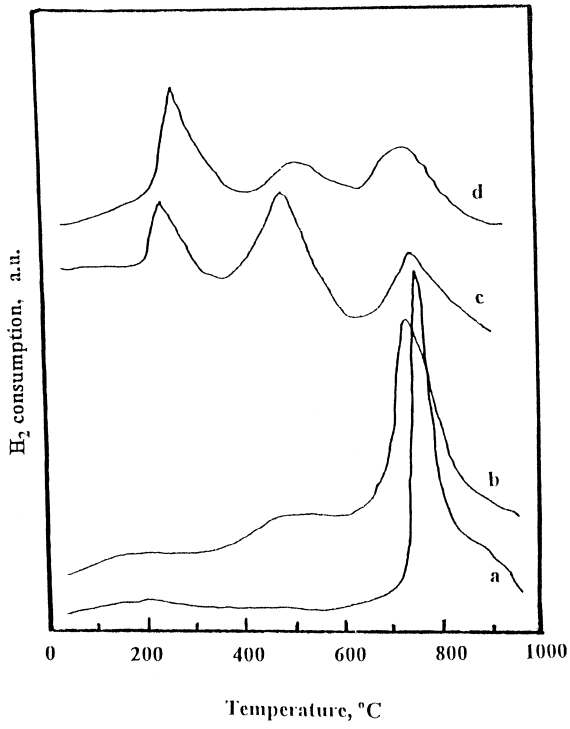

Fig. 1. TPR profiles of the γ-Al_2O_3 supported samples. (a) γ-Al_2O_3, (b) Fe/γ-Al_2O_3, (c) Pt/γ-Al_2O_3, (d) Pt–Fe/γ-Al_2O_3.

742°C was found in the γ-Al_2O_3 sample (Fig. 1a), which is considered to be the reduction of surface Al^{3+} on γ-Al_2O_3 [17]. The TPR profile of Fe/γ-Al_2O_3 (Fig. 1b) showed two peaks. The first peak at 480°C is assigned to the reduction of surface Fe^{3+} and the second peak at 720°C is attributed to the reduction of the γ-Al_2O_3 support. By comparing the reduction profiles of Fig. 1a and b, we can see that the addition of Fe to γ-Al_2O_3 caused the reduction peak of the γ-Al_2O_3 to shift to a lower temperature. There are three reduction peaks (240, 471, 738°C) in Fig. 1c, which is the TPR profile of the Pt/γ-Al_2O_3 catalyst. The first and second peaks are assigned to two different species of the highly dispersed Pt precursor (probably PtO_2), and the third peak is attributed to the γ-Al_2O_3 support. It is interesting to find that the addition of Pt to γ-Al_2O_3 decreased the area of the reduction peak of the latter, and this can be regarded as an indication of an interaction of Pt with the γ-Al_2O_3 support. The situation of the Pt–Fe/γ-Al_2O_3 sample (Fig. 1d) is approximately the same as that of the Pt/γ-Al_2O_3 (first peak: 266°C, second peak: 502°C, and third peak: 700°C). While the first peak and the third peak of the Pt–Fe/γ-Al_2O_3 sample can be unambiguously attributed to the reduction of Pt oxide and γ-Al_2O_3, respectively (by comparison with Fig. 1c and a), the temperature of the second peak is obviously higher than that of the second Pt peak in Fig. 1c and of the Fe peak in Fig. 1b. Since there are no more Pt or Fe peaks can be found in this temperature range, it is natural to visualized that this second peak in Fig. 1d was a species resulting from the interaction of Pt and Fe. Furthermore, on Fig. 1d, the third reduction peak temperature is 700°C, which is lower than that for the reduction of γ-Al_2O_3 in the Fe/γ-Al_2O_3, Pt/γ-Al_2O_3 and γ-Al_2O_3 samples, and this can be explained as the existence of an interaction between the metallic components (Pt and Fe) and the γ-Al_2O_3. Another interesting fact is that the reduction peaks of the iron components in the Fe/γ-Al_2O_3 and Pt–Fe/γ-Al_2O_3 samples are quite different from the TPR peak of bulk α-Fe_2O_3 [18]. All these results imply that there exist complicated interactions among the Pt, Fe and γ-Al_2O_3 in the Pt–Fe/γ-Al_2O_3 catalyst. The TPR profile

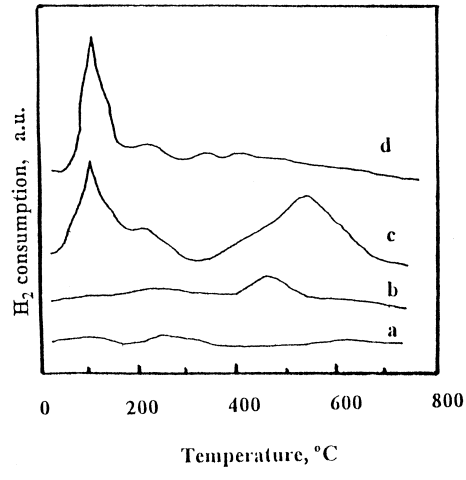

Fig. 2. TPR profiles of the SiO_2 supported samples. (a) SiO_2, (b) Fe/SiO_2, (c) Pt/SiO_2, (d) Pt–Fe/SiO_2.

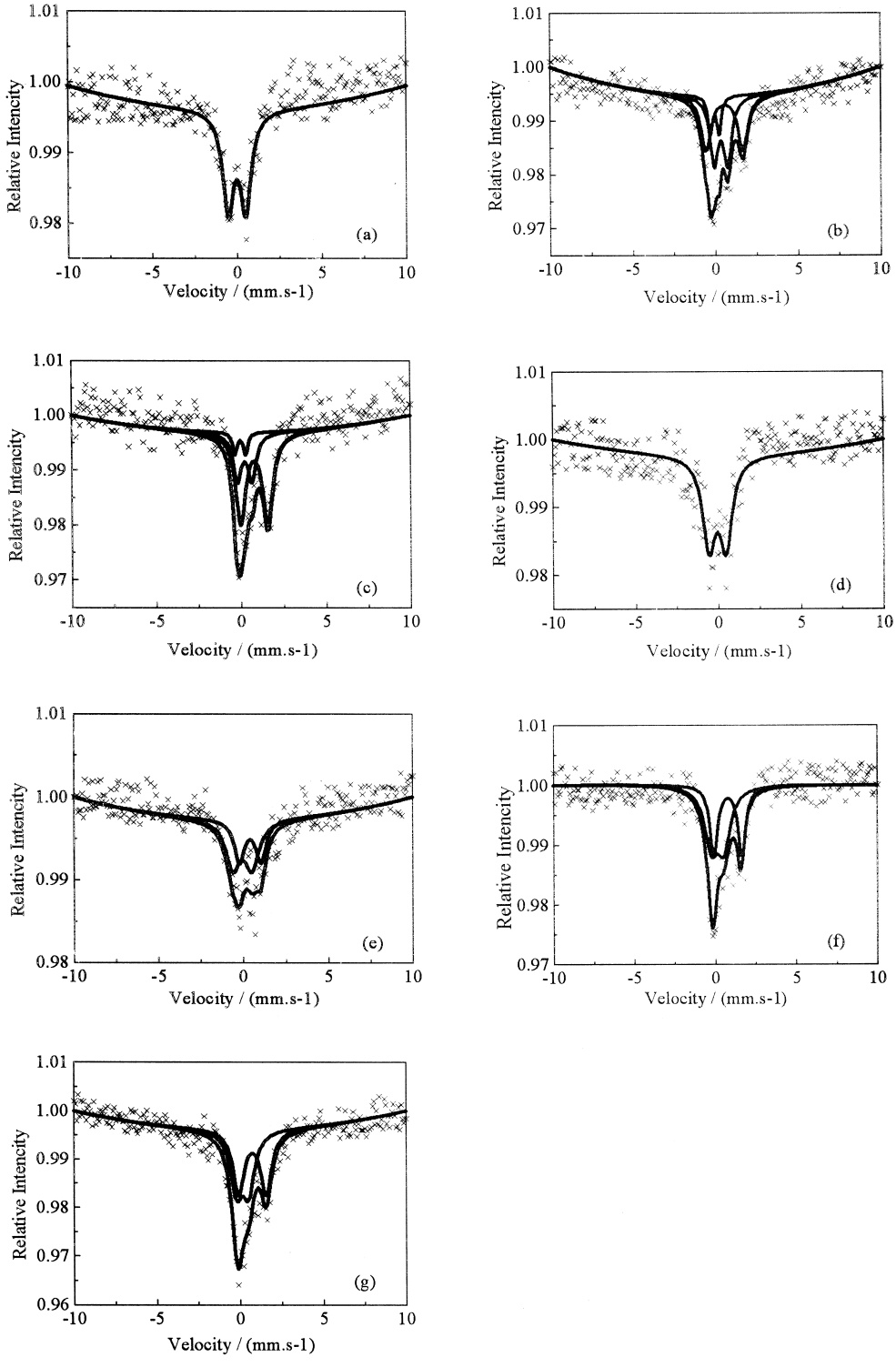

Fig. 3. In situ ^{57}Fe MBS of Fe/γ-Al_2O_3 and Pt–Fe/γ-Al_2O_3 in different reduction stages of TPR with H_2/N_2. (a) Fe/γ-Al_2O_3 before reduction, (b,c) first and second TPR peaks of Fe/γ-Al_2O_3, (d) Pt–Fe/γ-Al_2O_3 before reduction, (e,f,g) first, second and third TPR peaks of Pt–Fe/γ-Al_2O_3.

of Pt–Fe/γ-Al_2O_3 are very similar to Pt–Sn/γ-Al_2O_3 [17].

In our previous studies, the Pt–Fe/SiO_2 has been found to be a dehydrogenation catalyst with better activity than the Pt–Fe/γ-Al_2O_3 catalyst [15]. So it will be of interest to study also the TPR profiles of SiO_2, Fe/SiO_2, Pt/SiO_2 and Pt–Fe/SiO_2 samples correspondingly to what have been investigated for the γ-Al_2O_3 supported samples. The results of these investigations are given in Fig. 2. We can see that there are no reduction peaks for the SiO_2 sample (Fig. 2a). The Fe/SiO_2 sample (Fig. 2b) shows a reduction peak at 470°C, which is similar to that of the Fe/γ-Al_2O_3, and is also in good agreement with the results of Berry et al. [18], but again quite different from the TPR of bulk α-Fe_2O_3. The Pt/SiO_2 sample (Fig. 2c) exhibits reduction peaks at 118, 210 and 535°C, which are consistent with the results of Baris et al. [20]. The TPR peaks at 118 and 210°C can be attributed to Pt precursors similar to that of the first reduction peak in the Pt/γ-Al_2O_3 sample, while the peak at 535°C corresponds to the second peak of the Pt/γ-Al_2O_3 catalyst. It is quite interesting to observe that the Pt–Fe/SiO_2 sample (Fig. 2d) shows only one reduction peak at 128°C. In comparing Fig. 2d with c and b, we find that there are no reductions at temperature of 400–600°C in Fig. 2d. So it is clear that there is an interaction between Pt and Fe on Pt–Fe/SiO_2 catalyst and the interaction is related to SiO_2 support.

3.2. TPR–in situ ^{57}Fe MBS studies

In this section, we employed the TPR–in situ ^{57}Fe MBS method to study the catalysts by the changes of Fe in TPR processes.

3.2.1. TPR–in situ ^{57}Fe MBS studies of Fe/γ-Al_2O_3 and Pt–Fe/γ-Al_2O_3

From the above TPR results we can see that there are two or three different reduction stages in the Fe/γ-Al_2O_3 and Pt–Fe/γ-Al_2O_3 samples. Fig. 3 shows the in situ MBS results of Fe/γ-Al_2O_3 and Pt–Fe/γ-Al_2O_3 in different TPR stages. The MBS parameters can be found in Table 1.

For the Fe/γ-Al_2O_3 before reduction, the in situ MBS shows a pure doublet (Fig. 3a, IS 0.36 mm/s and QS 1.14 mm/s), which indicate that the Fe^{3+} species was highly dispersed on the γ-Al_2O_3 support before reduction. From the in situ MBS of the first TPR peak, it was calculated that 86% of the Fe^{3+} had been reduced to Fe^{2+} in tetrahedral vacancy and octahedral vacancy (Fig. 3b). Vaishnava et al. [21] have reported the formation of $FeAl_2O_4$ (Fe^{2+} in tetrahedral vacancy and octahedral vacancy) for

Table 1
Results of ^{57}Fe MBS for Fe/γ-Al_2O_3 and Pt–Fe/γ-Al_2O_3 in different reduction stages of TPR in H_2/N_2

Samples	TPR stage	IS (mm/s)	QS (mm/s)	Peak area (%)	Assignment
Fe/γ-Al_2O_3	Before reduction	0.36	1.14	100	Fe^{3+}
	First peak at 480°C	0.30	0.61	14	Fe^{3+}
		0.71	0.90	43	Fe^{2+}(T)
		0.95	2.48	43	Fe^{2+}(O)
	Second peak at 720°C	0.30	0.69	7	Fe^{3+}
		0.57	0.96	28	Fe^{2+}(T)
		1.19	1.96	65	Fe^{2+}(O)
Pt–Fe/γ-Al_2O_3	Before reduction	0.27	1.14	100	Fe^{3+}
	First peak at 266°C	0.27	1.24	61	Fe^{3+}
		0.79	1.41	39	Fe^{2+}(T)
	Second peak at 502°C	0.50	0.80	58	Fe^{2+}(T)
		1.11	1.93	42	Fe^{2+}(O)
	Second peak at 700°C	0.50	0.80	49	Fe^{2+}(T)
		1.15	1.82	51	Fe^{2+}(O)

a 14% Fe/γ-Al_2O_3 catalyst reduced in hydrogen at 673 K, and our Mössbauer parameters are close to their results. However, in which vacancy did the reduced Fe^{2+} come first is still unknown. For the second TPR peak of the Fe/γ-Al_2O_3, a total of 93% Fe^{3+} had been found to be reduced to the Fe^{2+}, and the content of Fe^{2+} in octahedral vacancy also increased (Fig. 3c). The fact that Fe^{3+} cannot be completely reduced to Fe^{2+} at the end of the TPR process can be explained by the strong interaction between Fe^{3+} and the γ-Al_2O_3 support.

For the Pt–Fe/γ-Al_2O_3, the in situ MBS before reduction also shows a pure doublet (Fig. 3d, IS 0.27 mm/s and QS 1.14 mm/s), which imply that the Fe^{3+} was in an oxidized state and was very similar to that of the Fe/γ-Al_2O_3 sample. In the in situ MBS spectrum of the first TPR peak at 266°C, 39% of the Fe^{3+} was reduced to Fe^{2+} in tetrahedral vacancy and no Fe^{2+} in octahedral vacancy was found (Fig. 3e). This implies that by adding Pt to the Fe/γ-Al_2O_3, the Fe^{2+} in tetrahedral vacancy can be formed at lower reduction temperatures. The second TPR peak at 502°C shows that 100% Fe^{3+} was reduced to Fe^{2+} in tetrahedral vacancy and octahedral vacancy (Fig. 3f). Finally, as the reduction temperature reached the third TPR peak, the Fe^{2+} in octahedral vacancy increased (Fig. 3g).

The results indicated that addition of Pt to Fe/γ-Al_2O_3 not only changed the TPR profile of the catalyst, but also enhanced its reducibility. No Fe^0 was found in the TPR processes of these two catalysts. In Section 3.1, it has been shown that the area of the second reduction peak in Fig. 1d decreased, which is explained as due to the interaction between Pt and Fe. This is confirmed by the TPR–in situ ^{57}Fe MBS measurements, which indicated that Fe co-existed with Pt in the 2+ valence on the γ-Al_2O_3 supported Pt–Fe catalyst.

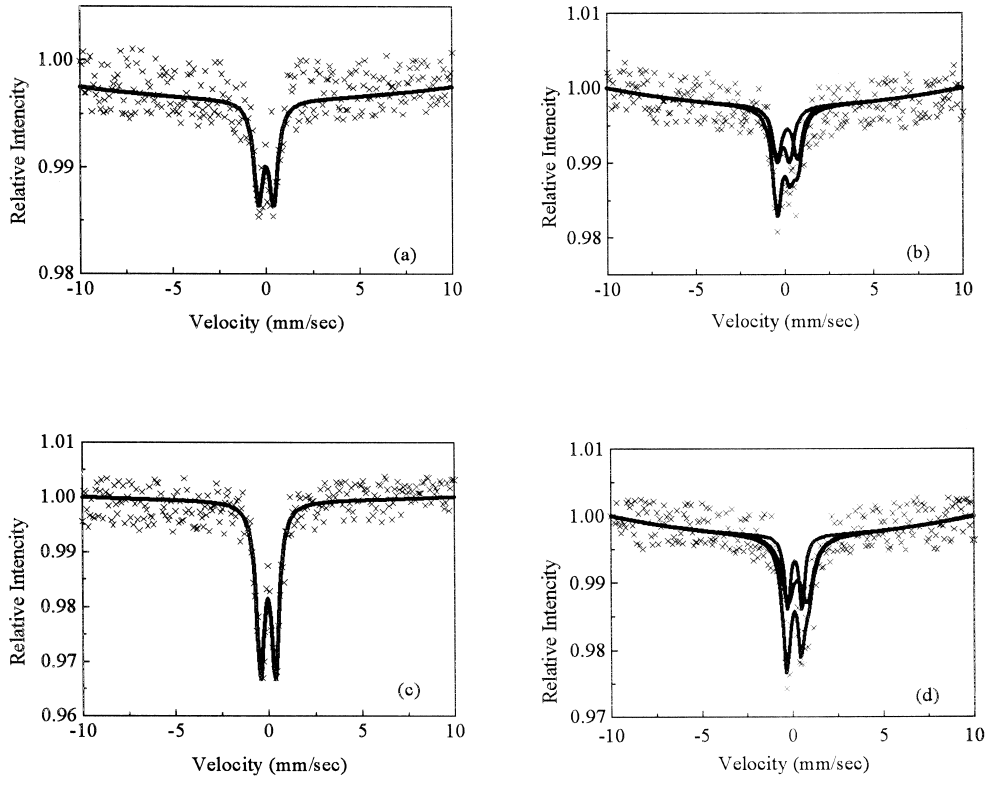

Fig. 4. In situ ^{57}Fe MBS of Fe/SiO_2 and Pt–Fe/SiO_2 in different reduction stages of TPR with H_2/N_2. (a) Fe/SiO_2 before reduction, (b) TPR peak of Fe/SiO_2, (c) Pt–Fe/SiO_2 before reduction, (d) TPR peak of Pt–Fe/SiO_2.

3.2.2. TPR–in situ ^{57}Fe MBS studies of Fe/SiO_2 and $Pt–Fe/SiO_2$

The TPR profiles of Fe/SiO_2 and $Pt–Fe/SiO_2$ samples in Fig. 2 show that there is only one reduction peak in each of the two samples. Fig. 4 shows the in situ MBS results of different reduction stages for the samples of Fe/SiO_2 and $Pt–Fe/SiO_2$. The MBS parameters are listed in Table 2.

For the Fe/SiO_2, the in situ MBS gave a pure doublet (Fig. 4a, IS 0.33 mm/s and QS 0.89 mm/s) before reduction. This means that Fe^{3+} was highly dispersed on the SiO_2 support before reduction and was similar to that on the $Fe/\gamma\text{-}Al_2O_3$. For the TPR peak of Fe/SiO_2, the in situ MBS indicated that 51% of Fe^{3+} was reduced to Fe^{2+} in tetrahedral vacancy (Fig. 4b), and no Fe^{2+} in octahedral vacancy was found in the TPR process. This result is very different from that of the $Fe/\gamma\text{-}Al_2O_3$.

Before reduction, the in situ MBS of $Pt–Fe/SiO_2$ also showed a pure doublet (Fig. 4c, IS 0.29 mm/s and QS 0.88 mm/s). For the in situ MBS of the TPR peak of $Pt–Fe/SiO_2$, 65% of Fe^{3+} was reduced to Fe^{2+} in tetrahedral vacancy (Fig. 4d), and again no Fe^{2+} in octahedral vacancy was found.

From the above discussions, we can note that the TPR–in situ MBS of the $Pt–Fe/SiO_2$ is different from that of the $Pt–Fe/\gamma\text{-}Al_2O_3$. The results indicated that addition of Pt to Fe/SiO_2 not only changed the TPR profile, but also increased the reducibility of Fe/SiO_2. Not any Fe^0 or Fe^{2+} in octahedral vacancy was found in the TPR processes in the both catalysts. From the TPR profiles we can know that there is an interaction between Pt, Fe and SiO_2. The TPR–in situ ^{57}Fe MBS results indicated that Fe co-existed with Pt in the 2+ valence on the SiO_2 support for $Pt–Fe/SiO_2$.

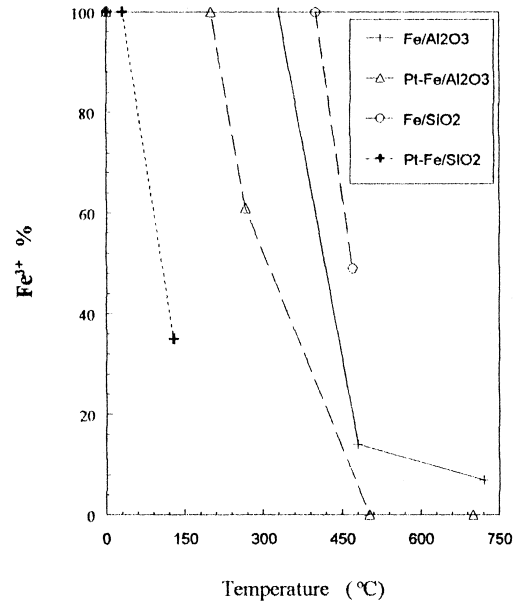

Fig. 5. Relationship between reducibility and temperature of the TPR profiles.

These Mössbauer results are in good agreement with XPS analysis [22].

Fig. 5 shows the change in percentage of Fe^{3+} at the TPR process on the above samples. It indicated that Fe^{3+} is more easily reduced to Fe^{2+} on $\gamma\text{-}Al_2O_3$ support than on SiO_2 support. Addition of Pt to $\gamma\text{-}Al_2O_3$ support not only

Table 2
Results of ^{57}Fe MBS for Fe/SiO_2 and $Pt–Fe/SiO_2$ in different reduction stages of TPR in H_2/N_2

Samples	TPR stage	IS (mm/s)	QS (mm/s)	Peak area (%)	Assignment
Fe/SiO_2	Before reduction	0.33	0.89	100	Fe^{3+}
	First peak at 470°C	0.25	0.78	49	Fe^{3+}
		0.51	1.26	51	Fe^{2+} (T)
$Pt–Fe/SiO_2$	Before reduction	0.29	0.88	100	Fe^{3+}
	First peak at 128°C	0.39	0.89	35	Fe^{3+}
		0.64	1.18	65	Fe^{2+} (T)

makes all Fe^{3+} to be reduced to Fe^{2+}, but also decreased the reduction temperature. Addition of Pt to the Fe/SiO_2 caused the reduction temperature to become lower, but this could not make all Fe^{3+} to be reduced to Fe^{2+}.

The Fe^{2+} can exist in tetrahedral vacancy and octahedral vacancy for γ-Al_2O_3 supported samples; The Fe^{2+} can exist in tetrahedral vacancy only for SiO_2 supported iron containing samples, and some Fe^{3+} were also found in this case. Many authors [23–26] have reported that on supported NiO, CoO, MoO_3 catalysts, etc., when the metal oxide content are very low, the cations enter into the tetrahedral vacancy of the support first. Our results indicated that Fe^{2+} can co-exist in tetrahedral vacancy and octahedral vacancy with Pt in the Pt–Fe/γ-Al_2O_3, while Fe^{2+} can co-exist with Pt only in tetrahedral vacancy for Pt–Fe/SiO_2. In our previous studies, we have found that the interaction of highly dispersed Pt species with the supporting materials could be further enhanced by incorporating onto the γ-Al_2O_3 a third component of metal oxides such as tin oxide [27]. In these circumstances, the Pt species was found to anchor on the support via the SnO promoter in the Pt–Sn/γ-Al_2O_3 bimetallic catalysts, constituting a 'sandwich' type structure. It is visualized that the existence of the 'sandwich' structure is an important factor for stabilizing the highly dispersed state of the Pt species, thus yielding improved activity, selectivity and stability for the catalysts in commercial hydrocarbon dehydrogenation processes. Thus, the interaction between Pt, Fe and the γ-Al_2O_3 or SiO_2 support for the Pt–Fe/γ-Al_2O_3 and Pt–Fe/SiO_2 catalysts can be visualized as that Pt species anchored on the support via the Fe^{2+} species in tetrahedral vacancy, and this seems to be the reason of high activities for dehydrogenation reactions over the Pt–Fe/γ-Al_2O_3 and Pt–Fe/SiO_2 catalysts.

Acknowledgements

This project was supported by the FORD and NSFC NO. 09412302, and by the Trans-century Training Program Foundation for the Talents by the State Education Commission of China.

References

[1] M.E. Kluksdahl, U.S, Patent 3 (1968) 415–737.
[2] G. Meitzner, G.H. Via, F.W. Lytle, S.C. Fung, J.H. Sinfelt, J. Phys. Chem. 92 (1988) 2925.
[3] G.M. Schwab, Disk, Faraday Soc. 8 (1950) 166.
[4] J.H. Sinfelt, Bimetallic Catalysis, Wiley, 1983.
[5] O.R. Short, S.M. Halid, J.R. Katzer, J. Catal. 72 (1981) 288.
[6] M.F.L. Johnson, V.M. Leroy, J. Catal. 35 (1974) 434.
[7] R. Bouwman, P. Biloen, J. Catal. 48 (1977) 209.
[8] W. Yang, L. Lin, Y. Fan, J. Zhang, Catal. Lett. 12 (1992) 267.
[9] K. Baalakrishnan, J. Shwank, J. Catal. 127 (1991) 287.
[10] R. Burch, J. Catal. 71 (1981) 348.
[11] B.A. Sexton, A.E. Hughes, K. Foger, J. Catal. 88 (1984) 466.
[12] N.W. Hurst, S.J. Gentry, A. Jones, Catal. Rev. -Sci. Eng. 24 (2) (1982) 233.
[13] R. Tang, S. Zhang, C. Wang, D. Liang, L. Lin, J. Catal. 106 (1987) 440.
[14] X. Ge, J. Shen, H. Zhang, Shince in China 39 (1) (1996) 53.
[15] J. Jia, Z. Xu, T. Zhang, L. Lin, J. Catal. 18 (2) (1997) 97, (in Chinese).
[16] R. Tang, R. Wu, L. Lin, Appl. Catal. 10 (1984) 163.
[17] W. Yang, R. Wu, L. Lin, J. Catal. 8 (4) (1987) 345, (in Chinese).
[18] F.J. Berry, L. Lin, C. Wang, R. Tang, S. Zhang, D. Liang, J. Chem. Soc., Faraday Trans. 1 81 (1985) 2293.
[19] M.A. Vannice, R.L. Garten, J. Mol. Catal. 1 (1996) 201.
[20] O.A. Baris, A. Holmen, E.A. Blekkan, J. Catal. 158 (1996) 1.
[21] P.P. Vaishnava, P.I. Ktorides, P.A. Montano, K.J. Mbadcam, G.A. Melson, J. Catal. 96 (1985) 301.
[22] J. Jia, Y. Kou, Z. Xu, T. Zhang, J. Niu, L. Lin, J. Catal. 18 (4) (1997) 263, (in Chinese).
[23] M. Lo Jacano, J. Phys. Chem. 75 (1971) 1044.
[24] L.W. Burggraf, D.M. Hercules, J. Catal. 78 (1982) 360.
[25] J.C. Vickerman, D.M. Hercules, J. Catal. 44 (1976) 404.
[26] D.S. Zingg, D.M. Hercules, J. Phys. Chem. 84 (1980) 2898.
[27] L. Lin, Huaxuetongbao 9 (1994) 14, (in Chinese).